Turbulent Boundary Layer with Injection and Surface Roughness

Joseph A. Schetz* and Brian Nerney†
Aerospace and Ocean Engineering Department
Virginia Polytechnic Institute and State University, Blacksburg, Va.

Experimental studies were conducted to measure directly the skin friction on an axisymmetric body with and without injection through the surface in a turbulent, low-speed flow. Measurements also were taken of velocity profiles and the axial turbulence intensity throughout the boundary layer. The axisymmetric model, with interchangeable solid, smooth and porous, slightly rough walls, was tested at Re_L from 4.96 to 6.11×10^6. Particular attention was paid to the law-of-the-wall region of the boundary layer. For both the law-of-the-wall and axial turbulent intensities, good correlation between the present experiment and previous experiment and theory was shown for the solid-wall data. Porous-wall tests with no injection showed an increase in the local skin friction and an attendant shift in the log region of the law-of-the-wall because of the slight roughness of the permeable-wall over the solid-wall values. For cases with blowing through the permeable wall, direct measurements of the skin friction showed a decrease over the unblown cases with the permeable wall. However, substantial blowing was required to reduce the skin friction below that obtained on the solid, smooth wall at the same conditions. The logarithmic region of the law-of-the-wall with blowing was found to be independent of the blowing rate over the range tested when compared to the porous, unblown wall results. These experimental data were used to construct extensions of both the Van Driest and Reichardt transport models. The Reichardt model proved more useful, and excellent results were achieved.

Nomenclature

A, A', B = constants in the law of the wall
A^+ = Van Driest damping factor
C_D = dissipation factor
k = roughness height
k^+ = ku_τ/ν
l, l_l = mixing lengths
q, Q = dynamic pressure
R = body radius
u = axial velocity
u_τ = $\sqrt{\tau_0/\rho}$
u^+ = u/u_τ
v_0 = injection velocity
v_0^+ = v_0/u_τ
y = distance from the wall
y^+ = yu_τ/ν
y_a^+ = Reichardt sublayer parameter
τ = shear
τ_0 = wall shear
ν = laminar kinematic viscosity
ρ = density
ϵ = eddy viscosity
δ = boundary-layer thickness
κ = $1/A'$

Introduction

TURBULENT flows over surfaces are of practical interest for a very wide range of engineering and scientific applications. Some of these applications involve cases where the surface is porous, so that fluid may be injected or withdrawn. Other cases involve evaporation or condensation, and here fluid appears to be injected or withdrawn through the interface. Thus, a detailed understanding of the nature of turbulent boundary layers with injection or suction is of great engineering importance. Some specific examples of practical applications include cooling of turbine blades; chemical processing; drying; and flows over forests, lakes, and the ocean.

The literature in this field is rich, and it is fortunate that recent review articles have summarized most of the previous work.[1-4] A number of experimental and theoretical studies (e.g., Refs. 5 and 6) have been directed at the near-wall region ($0 \le y/\delta \le 0.10$), and attempts (e.g., Refs. 5 and 6) have been made to generalize the "law of the wall," which is now well established for flows over solid surfaces,[7] at least for low-speed flows, to cases with injection or suction. Two of the more widely accepted suggestions are given as follows:

Stevenson Wall Law[5]

$$(2/v_0^+)\left[(1+v_0^+u^+)^{1/2}-1\right]=A\log(y^+)+B \tag{1}$$

Simpson Wall Law[6]

$$(2/v_0^+)\left[(1+v_0^+u^+)^{1/2}-(1+11.0\,v_0^+)^{1/2}\right]=A\log(y^+/11) \tag{2}$$

It is interesting and troublesome that these expressions do not agree with each other, and so they cannot both be correct. However, one expression seems to agree best with some data[8] and the other with other data.[6] This situation is very reminiscent of the confusion surrounding exterior turbulent boundary-layer flows in the later 1940's and early 1950's. That confusion can be traced to the lack of reliable and consistent skin friction data at that time. The whole picture was clarified by the introduction and application[9] of the skin friction balance for the direct measurement of wall shear. We believe that the current difficulties with turbulent boundary layers with injection and suction can be traced to the same source: unreliable and inconsistent wall shear data.

The whole matter is of more than academic interest, since the law of the wall is used directly in all turbulent transport modeling efforts. We can illustrate briefly by considering how

Received Nov. 5, 1976; revision received May 20, 1977.
Index category: Boundary Layers and Convective Heat Transfer – Turbulent.

*Professor and Department Head, Aerospace and Ocean Engineering Department. Associate Fellow AIAA.
†Graduate Assistant, Aerospace and Ocean Engineering Department; now at LTV, Dallas, Texas.

models of various types are derived for flows over solid surfaces. For simplicity and brevity, we discuss here only the logarithmic portion of the wall law. If we assume an eddy viscosity representation

$$\tau=\rho\epsilon(\partial u/\partial y) \tag{3}$$

then we take $\tau=\tau_0$ near the wall and use the wall law[7]

$$u/u_\tau=A'\ln(yu_\tau/\nu)+B$$
$$=A\log(yu_\tau/\nu)+B \tag{4}$$

to obtain $\partial u/\partial y$, and we can solve for

$$\epsilon=(l/A')u_\tau y \tag{5}$$

If one prefers a mixing length model

$$\tau=\rho l^2\left|\frac{\partial u}{\partial y}\right|\frac{\partial u}{\partial y} \tag{6}$$

the wall law gives

$$l=(l/A')y \tag{7}$$

The more complex models that have been introduced recently follow the same pattern. For example, near the wall, the turbulent kinetic energy equation simplifies to[10]

$$\tau=\rho\, C_D^{-1/2} l_l^2\left(\frac{\partial u}{\partial y}\right)^2 \tag{8}$$

and the wall law is used to yield

$$l_l=(C_D^{1/4}/A')y \tag{9}$$

All of these "models" – Eqs. (5, 7, and 9) – are used widely in numerical procedures to calculate turbulent boundary-layer flows for design and scientific processes.[10-13]

Since porous surfaces necessarily involve some roughness, this extra complication must be taken into account carefully. Thus, an important part of any injection (or suction) study must be a documentation of the flow over the surface of interest without injection or suction, so that the effects of the surface roughness can be displayed clearly. Also, further control tests where everything is the same except that the porous surface is replaced by a smooth, solid surface obviously will be useful.

In view of the preceding discussion, it is clear that accurate, direct measurements of wall shear in the presence of injection and suction are required, so that the development of basic understanding and predictive calculation procedures based on realistic models of turbulent transport in the near-wall region can proceed. We have undertaken a program of such measurements for cases with injection, and the apparatus, techniques, and results are described in the following sections. This is succeeded by a section wherein our experimental results are used to derive new models for turbulent transport in such cases.

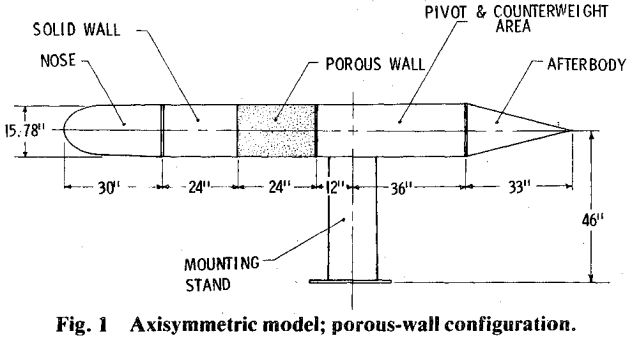

Fig. 1 Axisymmetric model; porous-wall configuration.

Experimental Studies

The testing was conducted in the Aerospace Engineering stability wind tunnel at speeds corresponding to 5, 7, and 9 in. of H_2O. This is a closed-circuit, continuous-flow facility with a 6- ×6-ft test section. The tunnel has the capability of achieving Reynolds numbers of the order of 10^6/ft with a low turbulence level of 1.08.

To undertake the task of experimentally measuring a turbulent boundary layer, an axisymmetric body with an ogive nose and a cylindrical main body was used (see Fig. 1). The circular cross section was chosen to eliminate corner effects or three-dimensional flows that have plagued some previous boundary-layer studies. The large diameter of 15.875 in. was chosen, so that possible transverse curvature effects would be minimized ($\delta/R=0.091$ to 0.098).

The 30-in.-long nose, shaped by the equation $r=2.6\,x^{0.33}$ and blended into zero slope at the base, was constructed of styrofoam and fiberglass and contains pressure taps around the circumference for aligning the model with the flow. The fiberglass was sanded and painted to a shiny finish that was smooth to the touch.

The testing area was designed to handle several configurations of solid and permeable wall testing. The first of the two configurations tested had a 4-ft-long, solid-wall, 0.5-in. wall thickness aluminum pipe that was machined smooth. The local skin friction measurements were made at a station 38.4 in. from the beginning of the testing area.

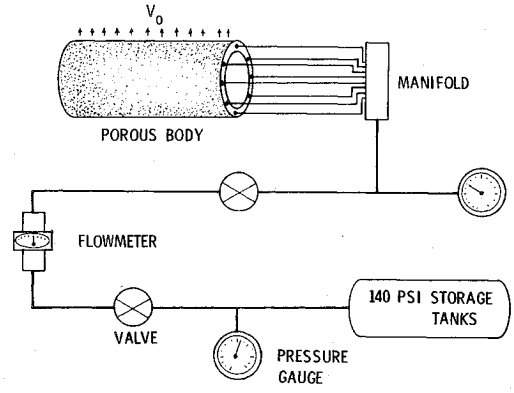

Fig. 2 Schematic of mass injection setup for the porous body.

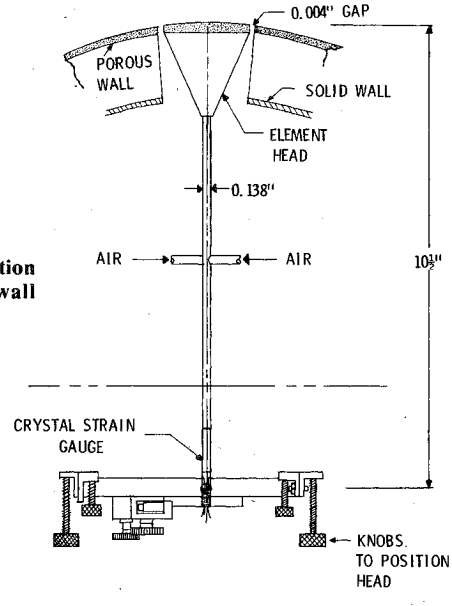

Fig. 3 Skin friction balance: porous-wall configuration.

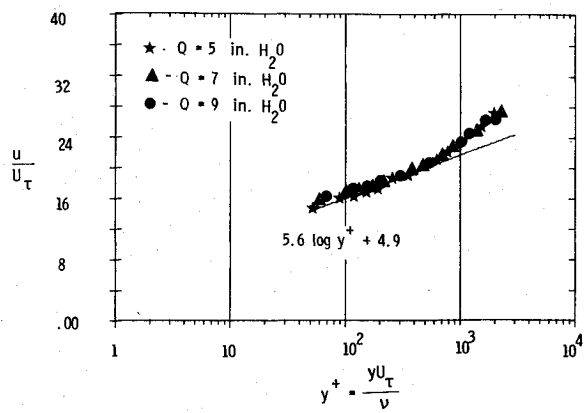

Fig. 4 Solid-body law-of-the-wall results for various tunnel speeds.

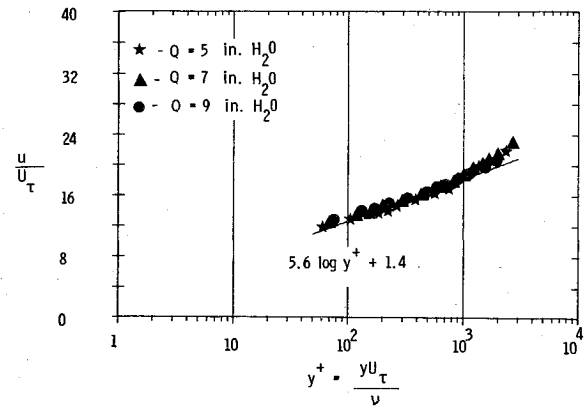

Fig. 5 Porous-body law-of-the-wall results for no injection at various tunnel speeds.

In the second configuration, the 4-ft-long, solid-wall testing area was replaced by a 2-ft, 0.5-in. wall thickness, aluminum solid-wall section, machined and matched to the nose with as much care as the 4-ft-long section, and a 2-ft-long, sintered, stainless-steel, porous-wall section. The finished product had a slightly rough feel, closely equivalent to a slightly used piece of aluminum oxide 400-J sandpaper. A 12-in.-diam solid tube then was placed inside the porous tube, and the assembly was sealed on each end with circular rings (Fig. 2). Holes were drilled in one of the rings for inlet air tubes. The capability for a floating element was incorporated by machining a circular hole in both the porous surface and inner aluminum surface and then preserving the seal of the porous canister by placing a closely machined tube in the hole (see Fig. 3). The flow uniformity from the porous canister was found to be good. It was checked with a hot wire and by touch. The regulation of input air was controlled and monitored with ball valves, two pressure gages, and a flowmeter as shown in Fig. 2.

The skin friction balance used for the wall shear measurements consisted of a special, highly sensitive crystal strain gage,‡ a 10-in.-long shaft that was used to increase sensitivity, the floating element head, and a mount for controlling the position of the element head. Figure 3 shows the balance setup for the porous-wall configuration. For both the solid- and porous-wall configurations, the balance was calibrated in the laboratory and in the model just before testing. The calibration curves agreed well and showed excellent linearity with little to no hysteresis. The porous-wall configuration was calibrated with and without blowing through the head, and no effect of blowing was found.

The pitot rake for velocity profile measurements was approximately 1½ in. high with one static port and 24 total pressure tubes staggered at increased spacing with increasing distance from the wall. The rake was mounted on the model at the same downstream location as the friction balance and slightly to one side to prevent damage to the balance. The turbulent intensity in the boundary layer was measured with a straight, constant-temperature hot wire.

Experimental Results

All the data taken are available in tabular form from the authors. The results discussed here are given in terms of law-of-the-wall plots, skin friction reduction as a function of mass transfer, and turbulence vs distance in the boundary layer.

The first test series that was performed employed the solid, smooth wall on the model. These tests were to validate all of the apparatus, instruments, and methods that were to be employed in the main tests and to serve as a reference base for skin friction reduction results. The complete test results are shown in Fig. 4 in terms of a conventional wall law plot. The excellent agreement with Clauser's suggestion for the logarithmic portion of the wall law can be noted. The data for

‡Available from Kistler-Morse, Inc.

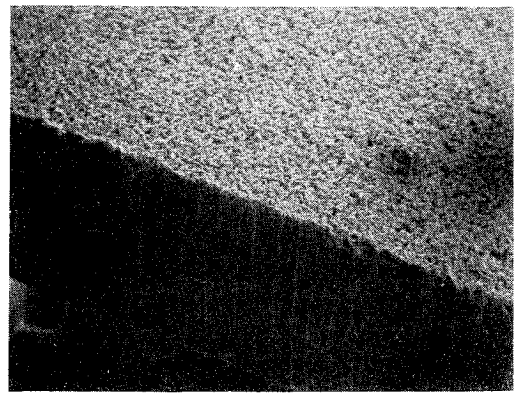

a) 20× magnification reduced to 60%.

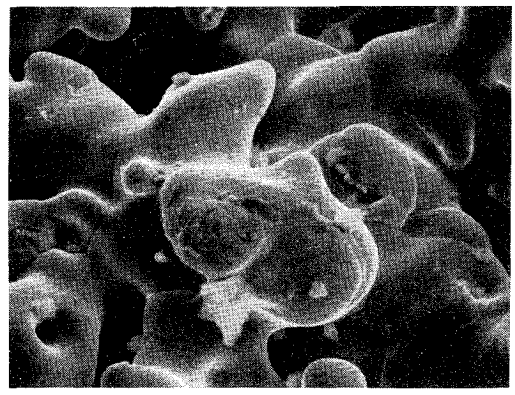

b) 1000× magnification reduced to 60%.

Fig. 6 Electron microscope photographs of the porous surface used in the experiments.

any one freestream velocity (i.e., q) show excellent coherence. The correlation of the data (various q's) with the Clauser wall law is equivalent to that for other workers.[7]

The next test series was run with the porous-wall section in place on the model but with no injection. These tests served to display the effects of the slight surface roughness that accompanies any porous surface. Wall law plot results are shown in Fig. 5. The logarithmic portion is shifted downward from the smooth, solid-wall results by an amount $\Delta(u^+) = 4.9 - 1.4 = 3.5$.

We have endeavored to compare our results thoroughly for these "roughness" effects tests with previous work. Clauser[7] has collected data for the wall law shift $\Delta(u^+)$ as a function of nondimensional roughness size $(k^+ \equiv ku_\tau/y)$ and roughness type. The matter is complicated, since the definition of roughness size and type remains imprecise, especially for small or intermediate roughness.[7] Our porous material was made from powdered stainless steel that con-

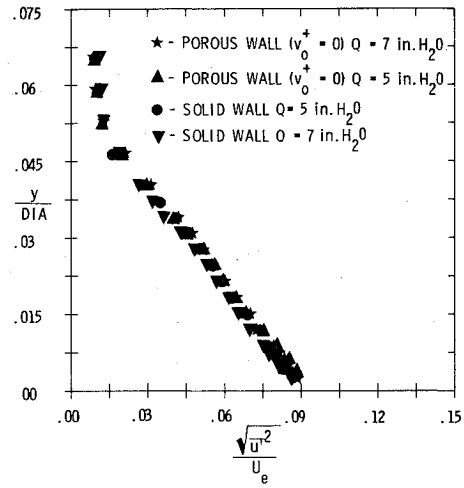

Fig. 7 $(\bar{u}^2)^{1/2}/u_e$ vs y/DIA. Comparison of solid- and porous-wall results (no injection).

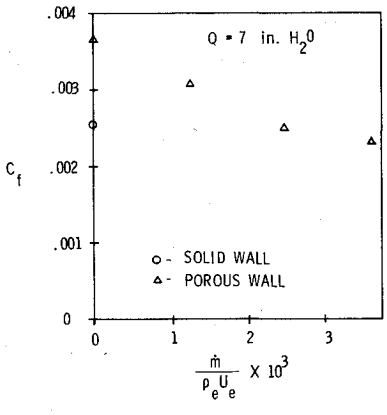

Fig. 8 Skin friction results for various blowing rates.

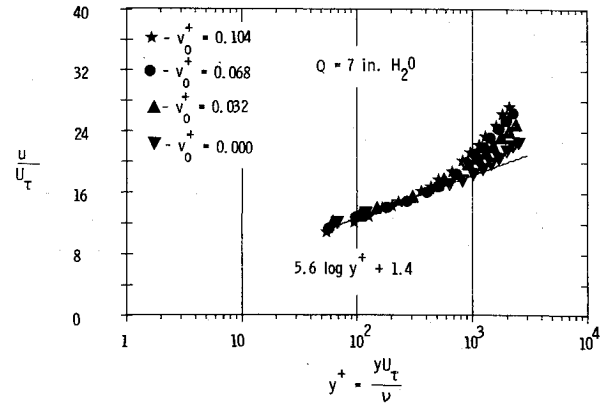

Fig. 9 Porous-body law-of-the-wall results for various blowing rates including $v_0^+ = 0.0$.

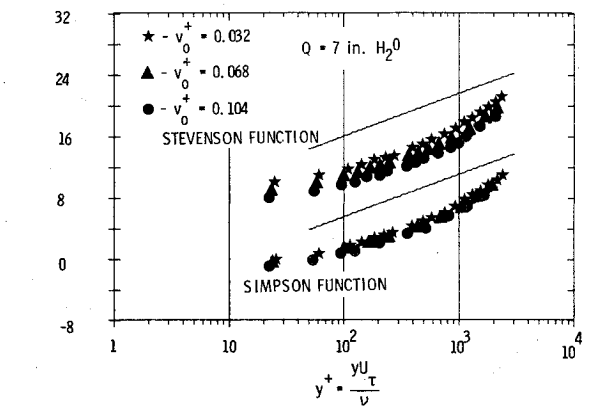

Fig. 10 Stevenson and Simpson function for various blowing rates.

sisted of 75% particles in the range of 40 to 70μ and 25% smaller particles. The particles are not spherical originally, and they are distorted somewhat in the sintering process. We have taken electron microscope photographs of the surface, and some examples are shown in Fig. 6. A maximum dimension of 70μ is typical. If one takes that as a definition of roughness size, then for our $q = 7$-in. H_2O test, as an example, we get $k^+ = 7$. Our observed $\Delta(u^+)$ shift for 3.5 is larger than that reported by Prandtl and Schlichting for "uniform" sand at that k^+. It does fall within the range of results that have been reported for mixtures of larger particles with uniform sand (see Fig. 11 of Ref. 7). Of course, the detailed shape of sand particles also is probably quite different from those of interest here, shown in Fig. 6. The turbulence intensity profiles measured across the boundary layer for the first two test series are shown in Fig. 7. These data are in excellent agreement with previous results[14,15] for these cases.

Finally, we come to the tests with injection. Some typical wall shear data are presented in Fig. 8. It can be seen clearly that the wall shear is decreased strongly with increasing injection rate. However, the wall shear on the porous wall without injection is substantially higher than that on the smooth, solid wall at the same test conditions. Considerable injection is required before one can reduce the wall shear below the solid, smooth-wall value. This result is very important for practical applications.

The results in terms of a wall law plot at $q = 7$-in. H_2O are shown in Fig. 9. The perhaps surprising result is that the logarithmic portion of the wall is unaffected by injection. The outer limit of the validity of the wall law can be seen to decrease with increasing injection rate. All of the data obtained (at various q and v_0^+) correlate with this single wall law with the same level of agreement as for the solid, smooth-wall cases.

These directly measured data are not in agreement with previously published, indirectly obtained data (e.g., Refs. 2-6). The primary area of disagreement is with regard to wall shear, which enters into the wall law plot through $u_\tau \equiv \sqrt{\tau_0/\rho}$. The older experiments inferred wall shear from either the slope of the velocity profile at the wall or the change in momentum thickness with streamwise distance. Both of these procedures were discredited long ago for the simpler cases with solid walls. Accurate wall shear data simply cannot be obtained in these ways with any reasonable reliability. On both practical and philosophical grounds, the directly measured wall shear data obtained here must be regarded as more accurate than any previously obtained by inference from measurements of other quantities. In this regard, it is important to restate that the older data do not agree among themselves.

The Stevenson and Simpson suggestions for the correct wall law including injection now can be tested against these new, directly measured data. This is shown in Fig. 10, where both can be seen to be deficient. Thus, any analytical models built using either of these functions also must be deficient.

The last data obtained and shown in Fig. 11 are the turbulence intensity profiles with injection. Clearly, the turbulence intensity is increased strongly by increasing injection rate. The results for the tests with injection may be summarized by stating that the skin friction is reduced sharply from the no-injection (porous-wall) value, and the turbulence intensity levels are increased strongly, but the wall law results in the logarithmic region are not changed by injection.

Development of Turbulent Transport Models

We have undertaken the development of new turbulent transport models for the near-wall region for cases with injection using our new experimental results. Since one can see from Eqs. (3, 6, and 8) that all types of turbulent transport models are related simply in this region, we have used an eddy

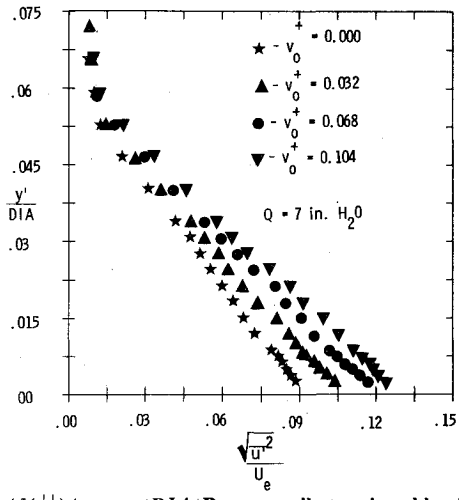

Fig. 11 $+(\bar{u}'^{\cup})/u_e$ vs y/DIA. Porous wall at various blowing rates.

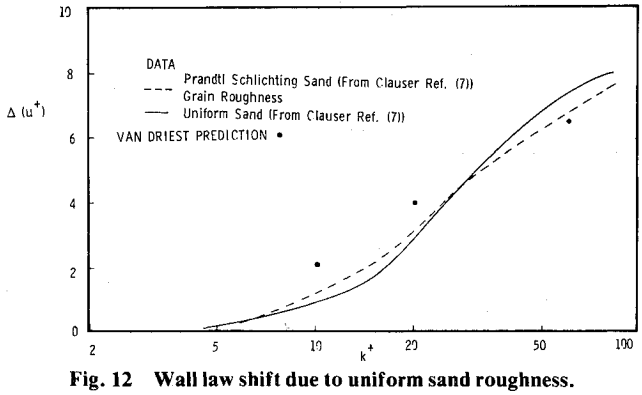

Fig. 12 Wall law shift due to uniform sand roughness.

viscosity formulation, Eq. (3), here. Of course, these specific results can be generalized easily to mixing length or *TKE* formulations.

In considering the whole near-wall region from the wall out through the logarithmic region, there are two general approaches: the "deductive" approach of Van Driest[16] and the "inductive" approach of Reichardt.[17] We shall attempt to apply both approaches to the new problem of interest here below.

Before attacking the injection problem, it is necessary to deal with the roughness attendant to porous surfaces even without injection through them. Our experimental results clearly show the importance of this effect. The effects of roughness by itself on the wall law have been presented by Clauser[7] in terms of a downward shift in the wall law $\Delta(u/u_\tau)$ vs the nondimensional roughness $k^+ \equiv ku_\tau/\nu$. Very importantly, roughness has been found to change the wall law only in the form

$$u/u_\tau = A' \ln(yu_\tau/\nu) + B - \Delta(u/u_\tau)$$
$$= A' \ln(yu_\tau/\nu) + B'(k_+) \qquad (10)$$

Thus the slope of the wall law, $\sim A'$, is not changed by roughness, and any realistic transport model must mirror this behavior. Van Driest,[16] in his original paper, suggested a method for taking the variation due to roughness into account:

$$l^+ = \kappa y^+ [1 - \exp(-y^+/26) + \exp(-60y^+/26k^+)] \qquad (11)$$

The second exponential in the brackets is the roughness term. He did not, however, test it against the uniform roughness data as collected by Clauser. We have done so, as shown in Fig. 12, where it can be seen that Van Driest's suggestion is not adequate.

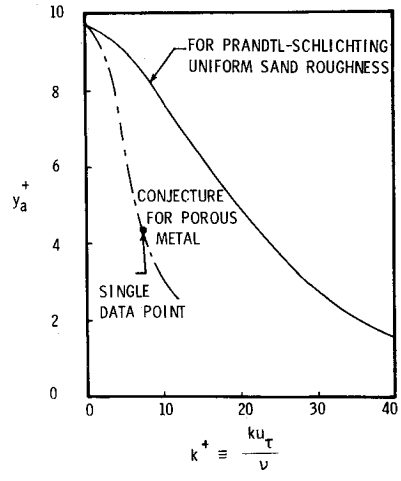

Fig. 13 Variation of the Reichardt sublayer to represent sand roughness effect.

The Reichardt model for no injection or suction

$$\rho\epsilon = \kappa\rho\nu[y^+ - y_a^+ \tanh(y^+/y_a^+)] \qquad (12)$$

has not been applied to rough-wall cases before. We have attempted the extension to such cases as follows. One can note that the only "free" quantity in the Reichardt model is y_a^+, which is a scale length of the order of the thickness of the laminar sublayer. If one wishes to have the Reichardt model fit the Clauser form of the wall law for smooth, solid walls [i.e., $A' = 2.43$ $(A = 5.6)$ and $B = 4.9$], then he must take $\kappa = 1/A' = 0.41$ and $y_a^+ = 9.7$. Now, it is reasonable to expect the thickness of the laminar sublayer, and thus also y_a^+, to decrease with increasing roughness. We have determined the variation $y_a^+(k^+)$ such that the correct shift $\Delta(u^+)$ is produced for the Prandtl-Schlichting uniform sand curve as an example. The required function $y_a^+(k^+)$ is shown in Fig. 13.

Since the shift $\Delta(u^+)$ that we observed on our rough surface was greater than that for uniform sand as reported by Prandtl and Schlichting, the uniform sand curve for $y_a^+(k^+)$ will not reproduce our results. It was found necessary to use $y_a^+ = 4.3$ to produce the observed $\Delta(u^+)$ shift. Thus, the "conjectured" curve in Fig. 13 through that single point is presented here only as a typical, hopefully useful, example. Separate functions, $y_a^+(k^+)$, apparently, will have to be developed for other specific types of roughness.

We are now in a position to attempt to include the effects of injection in both the Van Driest and Reichardt formulations. Consider first the Van Driest model extended to include roughness on an ad hoc basis, $f(k^+)$, such that the correct shift $\Delta(u^+)$ is obtained near the $k^+ = 7$ of interest here. The only influence of blowing should be on the damping factor A^+, and we therefore must look for $A^+(v_0^+)$ such that the Van Driest model will fit the wall law as determined from our experiments. Following the original development of Van Driest[16] but using now the momentum equation as

$$\tau = \tau_0 + \rho v_0 u \qquad (13)$$

there results

$$\frac{du^+}{dy^+} = \frac{2(1+v_0^+u^+)}{1+\sqrt{1+4\kappa^2(1+v_0^+u^+)(y^+)^2[1-\exp(-y^+/A^+)]f(k^+)}} \qquad (14)$$

The term $f(k^+)$ multiplying the exponent is the correction introduced here to produce the proper $\Delta(u^+)$ vs k^+ result

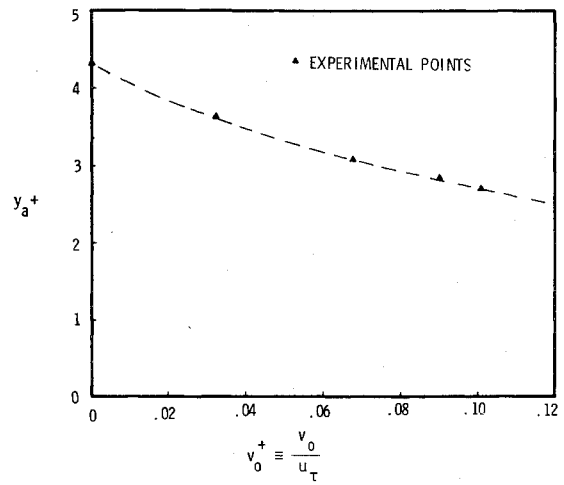

Fig. 14 Variation of the Reichardt sublayer parameter to reproduce experimental wall law with injection through a porous metal surface.

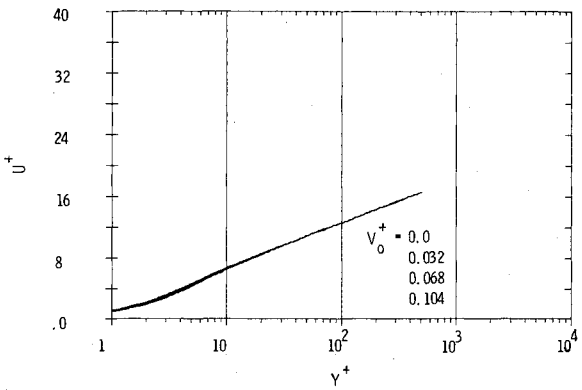

Fig. 15 Law-of-the-wall velocity profile predictions using the extended inductive model with blowing for the cases of the experiments.

for $k^+ \approx 7$. Choosing a representative value of y^+ and varying A^+ with v_0^+ so that the predicted value of $u^+(y^+)$ matches the experimental values, a surprising result is obtained. The Van Driest model cannot be adapted to produce a wall law in agreement with our experimental results! This can be seen from Eq. (14), since du^+/dy^+ in the log region remains a function of v_0^+ for large y^+ no matter how A^+ is made to vary with v_0^+. This behavior is contrary to what we have observed experimentally.

The basic Reichardt model is, fortunately, more flexible than the Van Driest model. If we wish to include blowing as well as roughness, we must look now for $y_a^+(k^+, v_0^+)$ such that our experimental wall law is reproduced. We already have found a complete $y_a^+(k^+, 0)$ for the simple case of uniform sand roughness and a conjectured curve for roughness of the type on our porous metal surface (see Fig. 13). Our experiments were at a single actual roughness size k that produced a nearly constant $k^+ = 7$. Since τ_0, and hence u_τ, varies with v_0, the value of k^+ varies with v_0^+ for a constant k. However, in our cases the variation of k^+ was only about 20%, which should be negligible.

With the generalized Reichardt model, the momentum equation becomes

$$\frac{du^+}{dy^+} = \frac{1 + v_0^+ u^+}{\{1 + \kappa(1 + v_0^+ u^+)[y^+ - y_a^+ \tanh(y^+/y_a^+)]\}} \quad (15)$$

The resulting $y_a^+(7, v_0^+)$ is shown in Fig. 14, and the success achieved in matching the behavior of our experimental wall law is shown in Fig. 15, which is to be compared to Fig. 9 in the log region $(6) \leq y^+ \leq 300)$. In order to determine the general function $y_a^+(k^+, v_0^+)$, further injection experiments will have to be run at other values of k^+ and with various types of wall roughness. We hope to do so in the future. In the interim, one probably can assume safely that the wall law for any combination of k^+ and v_0^+ may be found by using the $\Delta(u^+)$ as a function of k^+ as represented by one of the curves in Clauser's[7] collection and presuming that v_0^+ will not produce a further shift. This is what we observed experimentally for the conditions studied. The function $y_a^+(k^+, v_0^+)$ then can be found for the new conditions based upon this assumption as in the foregoing.

Conclusion

An axisymmetric model was designed and built for studying turbulent boundary layers including the capability of measuring local wall shear directly with injection. For the solid-wall configuration, the experiments gave good quantitative results for both the law of the wall and turbulent intensities when compared with well-established theory and data. This served to validate the apparatus, instruments, and procedures used.

For the no-blowing, porous-wall tests, the effect of surface roughness was seen to lower the intercept of the logarithmic portion of the law-of-the-wall region by 3.5, increase the local skin friction over the solid wall, and increase the axial turbulence level slightly. Blowing reduced the skin friction sharply; however, substantial blowing was required to reduce the skin friction below that obtained on the solid, smooth wall at the same conditions.

For the porous-wall tests with blowing, the logarithmic portion of the law-of-the-wall data correlation was seen to be independent of blowing rate, compared to the unblown, porous-wall results. This was for blowing rates that markedly reduced the skin friction over the case of the porous wall with no blowing.

The data were used to extend both the Van Driest and Reichardt wall region turbulent transport models to cases with injection and surface roughness. Van Driest's original suggestion for roughness proved inadequate, therefore an ad hoc "correction" that could be used for a small range of roughness near our experimental conditions was developed. The Van Driest model could not be made to represent our experimental observations correctly with blowing. Perhaps the basic notion used in his "deductive" development is not broad enough to encompass the phenomena accompanying injection. The Reichardt model, which is "inductive" in nature, is necessarily more flexible. Direct extensions to account for roughness and injection were developed.

Acknowledgment

This work was supported by the National Science Foundation under Grant GK43459. George Lea was the Grant Monitor.

References

[1] Baronti, P., Fox, H., and Soll, D., "The Turbulent Boundary Layer with Mass Transfer," *Astronautica Acta,* 1964.

[2] Jeromin, L.O.F., "The Status of Research in Turbulent Boundary Layers with Fluid Injection," *Progress in Aerospace Science,* Vol. 10, Pergamon Press, New York, 1970.

[3] Coles, D., "A Survey of Turbulent Boundary Layers with Mass Transfer," Rand Corp., Rept. P-4697, Sept. 1971.

[4] Kays, W.M. and Moffat, R.J., "The Behaviour of Transpired Turbulent Boundary Layers," *Studies in Convection,* Vol. 1, edited by B. Launder, Academic Press, New York, 1975.

[5] Simpson, R.L., "The Turbulent Boundary Layer on a Porous Wall," Ph.D. Thesis, Stanford Univ., 1968.

[6] Stevenson, T.N., "A Law of the Wall for Turbulent Boundary Layers with Suction or Injection," Cranfield College of Aeronautics, Rept. 166, Cranfield, England, July 1963.

[7] Clauser, F., "The Turbulent Boundary Layer," *Advances in Applied Mechanics,* Vol. 4, Academic Press, London, 1956, pp. 1-51.

[8] Schetz, J.A. and Favin, S., "Numerical Calculation of Turbulent Boundary Layers Including Suction or Injection with Binary Diffusion," *Astronautica Acta,* Vol. 16, Dec. 1971, pp. 339-352.

[9] Liepmann, H.W. and Dhawan, S., "Direct Measurements of Skin Friction in Low-Speed and High-Speed Flow," *Proceedings of the First U.S. Congress on Applied Mechanics,* 1951.

[10] Launder, B., *Mathematical Models of Turbulence,* Imperial College, London, England, 1975.

[11] Kline, S.J., Morkovin, M.V., Savran, G., and Cockrell, D.J., *Proceedings of the Computation of Turbulent Boundary Layers—AFOSR/IFP/Stanford Conference,* 1968.

[12] Bradshaw, P., Ferriss, D.H., and Atwell, N.P., "Calculation of Boundary Layer Development Using the Turbulent Energy Equation," *Journal of Fluid Mechanics,* Vol. 28, Pt. 3, 1967, pp. 593-616.

[13] Cebeci, T., "Calculation of Compressible Turbulent Boundary Layers with Heat and Mass Transfer," *AIAA Journal,* Vol. 9, June 1971, pp. 1091-1097.

[14] Rotta, J., "On the Theory of Turbulent Boundary Layer," NACA TM 1344, Feb. 1953.

[15] Schlicting, H., *Boundary Layer Theory,* McGraw-Hill, New York, 1968.

[16] van Driest, E.R., "On Turbulent Flow Near a Wall," *Journal of the Aeronautical Sciences,* Vol. 23, Nov. 1956, pp. 1007-1011.

[17] Reichardt, H., "Vollstandige Darstellung der Turbulentent Gerschwindigkeitsverteilung," *Glatten Leitungen,* Zeit. Angew. Math. Mech. XXXI, July 1951, pp. 208-219.